Available online at www.sciencedirect.com

ScienceDirect

Proceedings of the Combustion Institute 37 (2019) 1605–1614

Proceedings of the Combustion Institute

www.elsevier.com/locate/proci

Experimental and computational investigation of autoignition of jet fuels and surrogates in nonpremixed flows at elevated pressures

Gerald Mairinger [a], Alessio Frassoldati [b], Alberto Cuoci [b], Matteo Pelucchi [b], Ernst Pucher [c], Kalyanasundaram Seshadri [a,*]

[a] *Department of Mechanical and Aerospace Engineering, University of California at San Diego, La Jolla, CA 92093-0411, USA*

[b] *Dipartimento di Chimica Materiali, e Ingegneria Chimica "G. Natta", Politecnico di Milano, Piazza L. da Vinci 32, Milano 20133, Italy*

[c] *Institute for Powertrains and Automotive Technology, Vienna University of Technology, A-1040 Vienna, Gusshausstrasse 27–29/315, Austria*

Received 1 December 2017; accepted 27 June 2018
Available online 5 October 2018

Abstract

Experimental and computational investigations are carried out to elucidate the fundamental mechanisms of autoignition of surrogates of jet-fuels at elevated pressures up to 6 bar. The jet-fuels tested are JP-8, Jet-A, and JP-5, and the surrogates tested are the Aachen Surrogate made up of 80 % *n*-decane and 20 % 1,3,5-trimethylbenzene by mass, Surrogate C made up of 60 % *n*-dodecane, 20 % methylcyclohexane and 20 % *o*-xylene by volume, and the 2nd generation Princeton Surrogate made up of 40.4 % *n*-dodecane, 29.5 % 2,2,4-trimethylpentane, 7.3 % 1,3,5-trimethylbenzene and 22.8 % *n*-propylbenzene by mole. Using the counterflow configuration, an axisymmetric flow of a gaseous oxidizer stream, made up of a mixture of oxygen and nitrogen, is directed over the surface of an evaporating pool of a liquid fuel. The experiments are conducted at a fixed value of mass fraction of oxygen in the oxidizer stream and at a fixed value of the strain rate. The temperature of the oxidizer stream at autoignition, T_{ig}, is measured as a function of pressure, p. Experimental results show that the critical conditions, of autoignition of the surrogates are close to that of the jet-fuels. Overall the critical conditions of autoignition of Surrogate C agree best with those of the jet-fuels. Computations were performed using skeletal mechanisms constructed from a detailed mechanism. Predictions of the critical conditions of autoignition of the surrogates are found to agree well with measurements. Computations show that low-temperature chemistry plays a significant role in promoting autoignition for all surrogates. The low-temperature chemistry, of the component of the

* Corresponding author.
E-mail address: seshadri@ucsd.edu (K. Seshadri).

https://doi.org/10.1016/j.proci.2018.06.224

surrogate with the greatest volatility, was found to have the most influence on the critical conditions of autoignition.

Keywords: Autoignition; Surrogate fuels; Jet fuels; Low temperature chemistry; Kinetic modeling

1. Introduction

Improved understanding of the combustion of jet-fuels at elevated pressures is essential for accurate predictions of chemical processes taking place in air-breathing propulsion systems. Jet-fuels are mixtures of numerous aliphatic and aromatic compounds. It has been established that a useful approach to obtain fundamental understanding of combustion of jet-fuels is to first develop surrogates that reproduce selected aspects of combustion of these fuels [1]. Numerous experimental, computational and analytical studies have addressed combustion of jet-fuels, surrogates of jet-fuels, and high-molecular weight hydrocarbon fuels at elevated pressures [2–8]. These studies include measurements and prediction of combustion processes in homogeneous systems at normal and elevated pressures [2–5], extinction of counterflow nonpremixed flames [7], autoignition in nonpremixed flows [6,9–11], and laminar premixed flames [12]. There are, however, very limited studies on autoignition of jet-fuels in nonuniform flows and at elevated pressures. The present study addresses this deficiency, and is focused on elucidating the mechanisms of autoignition of surrogates of jet-fuels at elevated pressures up to 6 bar. Autoignition is an important property that has a significant influence on performance of compression-ignition engines. The present studies are carried out in nonpremixed systems because it best describes autoignition and combustion in compression-ignition engines.

Experimental and computational investigations were carried out recently to elucidate the fundamental mechanism of autoignition of *n*-heptane, *n*-decane, and *n*-dodecane in nonpremixed flows at elevated pressures up to 6 bar [8]. The results showed that *n*-dodecane is most easy to ignite followed by *n*-decane and *n*-heptane. This was in agreement with previous experimental and computational studies at 1 atm where a similar order of reactivities for these fuels were observed at low strain rates [11,13]. A noteworthy finding was that low-temperature chemistry played a dominant role in promoting autoignition [8]. The influence of low-temperature chemistry was found to increase with increasing pressure [8]. The present study extends this to jet-fuels and its surrogates.

2. Experiment

Experimental and computational studies are carried out employing the counterflow configuration wherein a cylindrical duct is placed 12 mm above an evaporating pool of a liquid fuel. From this duct an axisymmetric flow of a gaseous oxidizer stream, made up of a mixture of oxygen (O_2) and nitrogen (N_2), is directed toward the surface of the liquid fuel. At the exit of the duct, the magnitude of the injection velocity is V_2, the temperature T_2, the density ρ_2, and the mass fraction of oxygen $Y_{O_2,2}$. Here subscript 2 represents conditions at the oxidizer-boundary. The temperature at the liquid-gas interface is T_s, and the mass averaged velocity on the gas side of the liquid-gas interface, as a result of evaporation of the liquid fuel, is V_s. Here subscript s represents conditions on the gas side of the liquid-gas interface. A stagnation plane is formed near the liquid-gas interface. It has been shown previously [11] that the radial component of the flow velocity at the liquid-gas interface is small and can be presumed to be equal to zero. A thin boundary-layer is established at the liquid-gas interface in the asymptotic limit of large Reynolds number, calculated using V_2, the kinematic viscosity of the oxidizer stream at the exit of the duct, and the distance, L, between the exit of the duct and the liquid-gas interface. The inviscid flow outside this boundary-layer is rotational, and the local strain rate, a_2, in the inviscid region evaluated at the stagnation plane, obtained from integration of Euler's equations, is $a_2 = 2V_2/L$ [11,14].

All gaseous streams are controlled by computer regulated analog mass flow controllers. A Pt-Pt 13 % Rh thermocouple with a wire diameter of 0.127 mm and a junction diameter of 0.21 mm is used to measure the temperature of the oxidizer stream, T_2. The measured temperatures are corrected to account for heat losses by radiation from the theromocouple wires [15]. Fuel is supplied to a fuel cup by a syringe pump with a volumetric flow accuracy of ± 0.01 mL/min. The temperature of the fuel entering the cup, T_c, is measured by a thermocouple. Further details of the burner including the procedure employed to maintain the level of the liquid fuel in the cup are described in detail elsewhere [7,8]. Experiments are conducted with the counterflow burner placed inside the High Pressure Combustion Experimental Facility (HPCEF)

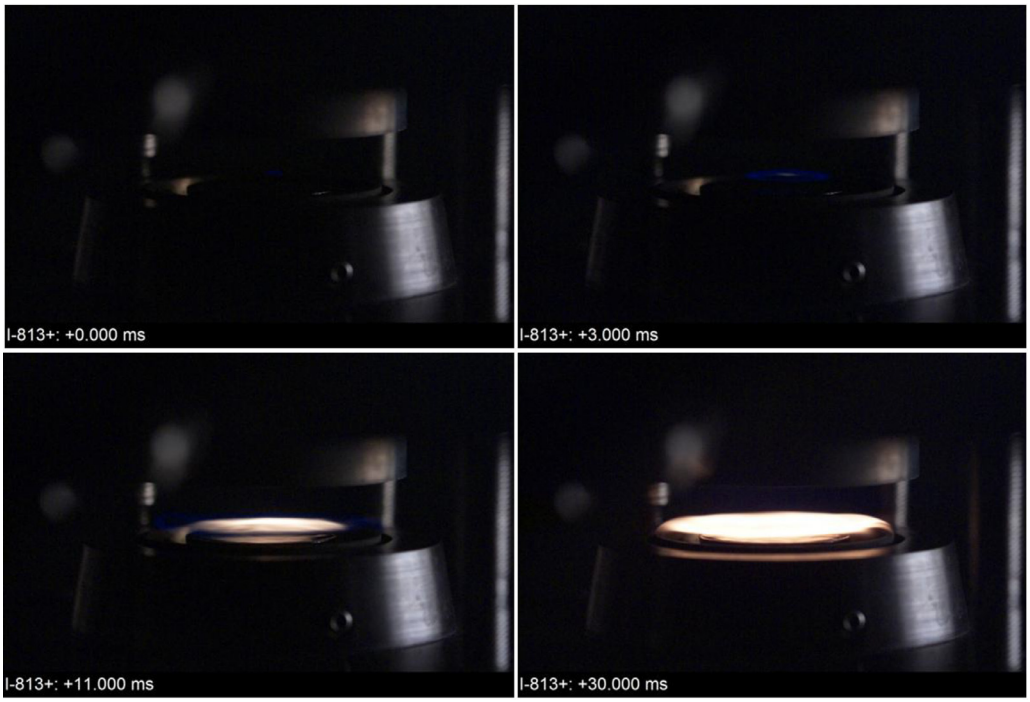

Fig. 1. High speed photograph of a typical autoignition event at $p = 4$ bar, $Y_{O_2,2} = 0.15$, $a_2 = 138\ s^{-1}$, and $T_2 = 1101$ K. The fuel is Jet-A.

described elsewhere [7,16,17]. The reactive flow field is characterized by the values of $Y_{O_2,2}$, T_2, a_2, and pressure, p. The experiments were conducted with $Y_{O_2,2} = 0.15$ and $a_2 = 138^{-1}$s. The temperature of the oxidizer stream at autoignition, T_{ig}, was measured as a function of p. The values of $Y_{O_2,2}$ and a_2 were selected to minimize rates of soot formation.

The procedure for measuring critical conditions of autoignition is as follows. First the desired chamber pressure is established by introducing nitrogen into the chamber. Water cooling systems are activated. The flowfield is established at the selected values of Y_{O_2}, and a_2 and at a value of T_2 that is less than T_{ig}. Liquid fuel is introduced into the fuel-cup and the syringe pump is used to control its level. The temperature of the oxidizer stream is gradually increased in small increments, allowing sufficient time for the system to reach steady-state, until autoignition takes place. The onset of autoignition is recorded using a high speed video camera operating at 1000 frames per second. Figure 1 shows the progression of the autoignition event at successive values of the time, t, recorded by the high speed camera. The first image is the start after the critical conditions have been reached, the second image, at 3.0 ms, shows a faint glow where the flame is seen as a small circular disc around the axis of symmetry. In the subsequent images the diameter of the flame increases. The repeatability of the measurements of T_{ig} is ± 5 K. The accuracy is estimated to be 15 K and is attributed to uncertainties in evaluating the correction that must be applied to the measured temperature due to heat losses from radiation from the thermocouple. Only those experimental data where autoignition is observed to take place close to the axis of symmetry is included in the data set. These measurements are performed for different values of p.

3. Fuels tested

The jet-fuels tested are JP-8, Jet-A, and JP-5, and the surrogates tested are the Aachen Surrogate, Surrogate C, and the 2nd generation Princeton Surrogate. The Aachen Surrogate is made up of 80 % n-decane and 20 % 1,3,5-trimethylbenzene by mass (H/C 2.00). This surrogate has been used in studies described in Ref. [7,9,10,18–20]. It accurately reproduced critical conditions of autoignition of JP-8 at nonpremixed conditions at atmospheric pressure [9,10], critical conditions of extinction of JP-8 at premixed and nonpremixed conditions at atmospheric pressure [9,10,20], and soot formation at nonpremixed conditions at atmospheric pressure [9]. Kinetic modelling studies have been carried using detailed chemical-kinetic mechanisms [9,10,20]. Surrogate C is made up of 60 % n-dodecane, 20 % methylcyclohexane

and 20 % *o*-xylene by volume (H/C 1.92). This surrogate has been used in studies described in [10,19–21]. It has been found to accurately reproduce at atmospheric pressure, critical conditions of autoignition of JP-8 at nonpremixed conditions [10,21], and critical conditions of extinction of JP-8 at nonpremixed and premixed conditions [10,20,21]. The 2nd generation Princeton Surrogate is made up of 40.4 % *n*-dodecane, 29.5 % 2,2,4-trimethylpentane, 7.3 % 1,3,5-trimethylbenzene and 22.8 % *n*-propylbenzene by mole (H/C = 1.96). It has been used in studies described in [2,3,7]. It has been found to accurately reproduce various aspects of combustion of jet fuels that include ignition delay times measured employing shock tubes and rapid compression machines [2,3], laminar burning velocities of premixed flames and critical conditions of extinction of diffusion flame at atmospheric pressure [2], and critical conditions of extinction of JP-8 at moderate pressure [7].

4. Formulation

Kinetic modelling described here is carried out using a skeletal mechanism made up of kinetic steps selected from the POLIMI detailed chemical-kinetic mechanism [22] that describes pyrolysis, partial oxidation and combustion of kerosene and aviation fuels. This skeletal mechanism is made up of 231 species and has been employed previously to characterize combustion of many surrogate mixtures proposed for kerosene [22]. Reference compounds in kerosene surrogates typically include *n*-alkanes, *iso*-alkanes, methylcyclohexane, aromatics (from toluene up to C_9 aromatics), decalin and tetralin. The kinetic steps for these compounds are included in the kinetic mechanism, and have been tested [22]. The kinetic subset for methylcyclohexane was updated from that in [23] in view of recent experimental measurements of ignition delay times in rapid compression machines at high pressure and low to intermediate temperatures [24]. Details of the revision and tests of the predictions of the updated kinetic mechanism for methylcyclohexane are provided a supplementary material.

The computations were performed with the OpenSMOKE++ code [25]. The structure of the reactive flow-field is obtained by solving the conservation equations of mass, momentum and energy, and the species balance equations. At the exit of the duct, the values of V_2, and the mass flux of O_2 and N_2 are specified, and the radial component of the flow velocity is presumed to be equal to zero. At the liquid-gas interface, mixed boundary conditions are applied for the species balance equations, and the energy conservation equation [8,13]. The temperature at the liquid-gas interface is obtained using Raoult's Law [26]. Empirical coefficients for calculating the vapor pressure, and the heat of vaporization, for these fuels are given in [27]. Simulations are performed, with $Y_{O_2} = 0.15$, $a_2 = 138\,s^{-1}$, and for p between 3 bar and 6 bar, using a computational grid with more than 400 grid points to ensure grid insensitive results. A converged non-reactive (cold) solution is first obtained for $T_2 = 300$ K. The temperature of the oxidizer stream is increased at a rate of 10 K/s until autoignition takes place and a hot flame is established. Numerical analyses showed that the predicted T_{ig} is not affected by the rate of temperature increase if it does not exceed 100 K/s. For the given value of p, autoignition is defined to take place at the value of $T_2 = T_{ig}$, where an abrupt transition takes place from a weakly reactive region to a flame.

5. Results

Figure 2 shows the measured temperature of the oxidizer stream at autoignition, T_{ig}, as a function of p, for JP-8, Jet-A, JP-5, the Aachen Surrogate, Surrogate C, and the Princeton Surrogate. For all fuels, T_{ig} decreases with increasing pressure. The values of T_{ig} for Surrogate C and the Princeton Surrogate agree best with those for the jet-fuels at pressures around 3 bar while at pressures close 6 bar, the values of T_{ig} for Surrogate C and the Aachen Surrogate agree well with those for the jet-fuels. Overall the critical conditions of autoignition of Surrogate C agree best with those for the jet-fuels.

Figures 3, and 4 show the predicted axial temperature distribution in the flow-field as a consequence of gradual increase in the value of T_2. In these figures results are shown at $p = 6$ bar, because at this pressure the role of low-temperature chemistry and the negative temperature regime are displayed best. Moreover at this pressure the values of T_{ig} for the surrogates differ the most. Figure 3 shows that for T_2 around 700 K, there is a small, but sudden, increase in the value of the temperature of the flow-field near the surface of the liquid pool, especially for the Aachen Surrogate (marked as LT in Fig. 3), indicating that low-temperature ignition has taken place. This is followed by the negative-temperature coefficient region (NTC) and "hot"-ignition.

Figure 4 shows the temperature increment ΔT [K] and temperature at the liquid-gas interface, T_s, as a function of T_2 for the surrogates. The quantity ΔT is the difference between the peak value of the temperature in the mixing layer and T_2. For the Aachen Surrogate, as T_2 is increased, a weakly reactive region appears in the vicinity of 700 K, that is marked by an increase in the value of ΔT followed by a decrease. Further increase in T_2 leads to a rapid rise in ΔT. This behavior is similar to that shown in Fig. 3. The temperature rise in the weakly reacting region is indicative of low-temperature ignition followed by the NTC region and finally "hot"-ignition

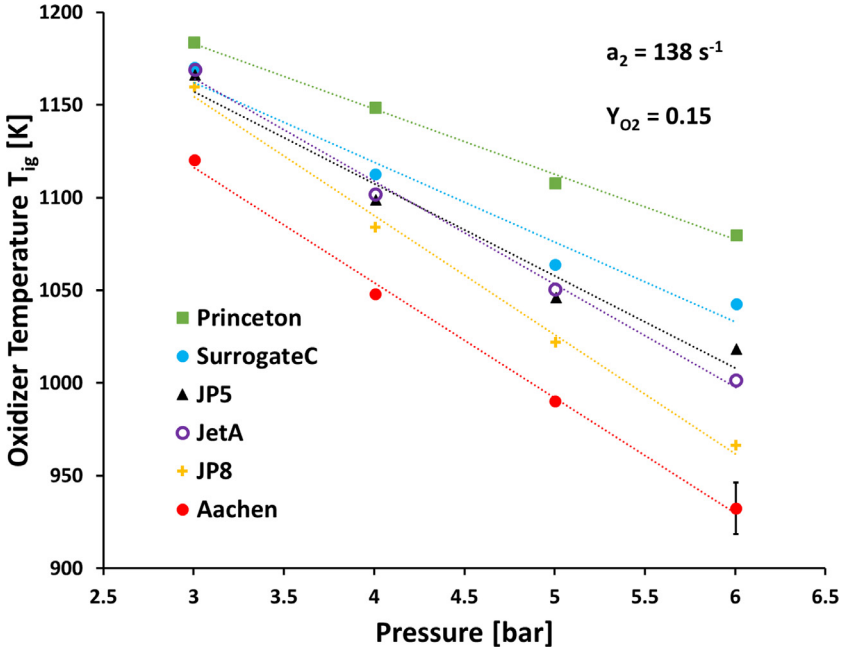

Fig. 2. The measured temperature of the oxidizer stream at autoignition, T_{ig} as a function of pressure, p, at $a_2 = 138\,s^{-1}$, and $Y_{O_2,2} = 0.15$. The symbols represent experimental data and the lines best fit to the experimental data. The error bar shown on one experimental data applies to all.

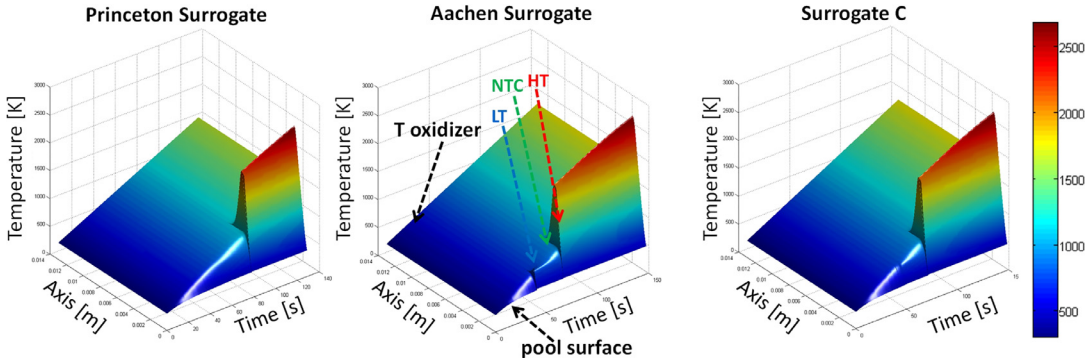

Fig. 3. Predicted axial temperature distribution in the flow-field of the surrogates, as a consequence of a gradually increasing the temperature of the oxidizer stream. The calculations were made at $p = 6$ bar, $Y_{O_2,2} = 0.15$, and $a_2 = 138\,s^{-1}$.

marked by large increase of ΔT. The higher reactivity of the Aachen Surrogate when compared to the other surrogates tested here is a consequence of its large paraffinic content namely *n*-decane that was found in previous studies [8] to exhibit significant low-temperature chemistry and NTC behavior. Figure 4 shows that T_s for all surrogates increases with increasing T_2 and its value is less than their respective boiling point temperature, about 30 K lower at the onset of low-temperature ignition and 20 K at the onset of "hot" ignition. The increase in the value of T_s with increasing temperature of the oxidizer stream is a consequence of the balance between the vapor-pressure and rates of vaporization. Raising the temperature of the oxidizer stream enhances the heat flux to the liquid pool that leads to higher values of T_s and the rates of evaporation. The boiling points for the Aachen Surrogate, Surrogate C, and the Princeton Surrogate at pressure of 1 bar is 446 K, 411 K, and 412 K, respectively and at a pressure of 6 bar, it is 532 K, 501 K, and 502 K, respectively. For the jet fuels JP-8 and Jet-A the value of the boiling point at 1 bar is roughly 500 K. The presence of cool flames, NTC behavior and two-stage ignition was also observed in previous experimental and computational stud-

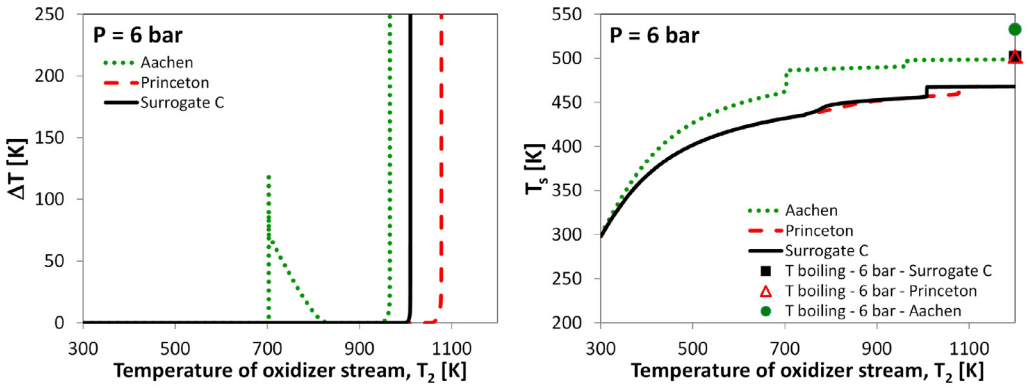

Fig. 4. Temperature increment ΔT [K], temperature at the liquid-gas interface, T_s, as a function of the temperature of the oxidizer stream, T_2, for $p = 6$ bar, $Y_{O_2,2} = 0.15$, and $a_2 = 138\ s^{-1}$.

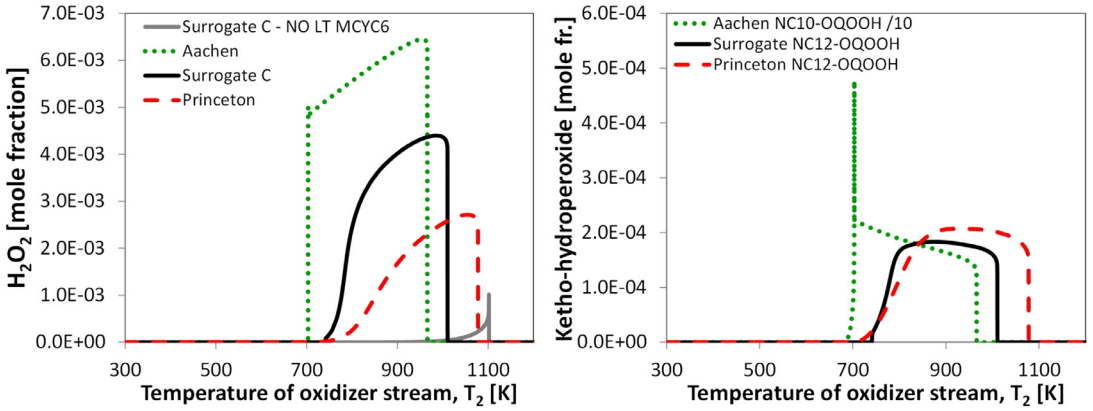

Fig. 5. Mole-fraction of hydrogen peroxide (H_2O_2), $X_{H_2O_2}$, and mole-fraction of keto-hydroperoxide (KET), X_{KET}, as functions of the temperature of the oxidizer stream, T_2, for $p = 6$ bar, $Y_{O_2,2} = 0.15$, and $a_2 = 138\ s^{-1}$. KET is marked as OQOOH.

ies of autoignition of *n*-heptane, *n*-decane, and *n*-dodecane in counterflow configuration and isolated fuel droplets [8,28,29].

Figure 5 shows the mole-fraction of hydrogen peroxide (H_2O_2), $X_{H_2O_2}$, and mole-fraction of keto-hydroperoxide (KET), X_{KET}, as functions of T_2. For all surrogates, H_2O_2 and KET are formed at the onset of low-temperature ignition and their concentration becomes negligible at the onset of "hot" ignition. Thus, for all surrogates 'hot'-ignition is preceded by low-temperature ignition. For purposes of illustration, computations were also done for Surrogate C, with kinetic steps characterizing low-temperature chemistry for methylcyclohexane removed. Figure 5 shows that as a consequence of this removal, the formation of H_2O_2 at low temperature is suppressed and H_2O_2 is formed in lower amounts only prior to the "hot"-ignition. Thus low-temperature ignition of Surrogate C comes primarily from methylcyclohexane in Surrogate C. Computations show that for the surrogates, the exothermic reaction zone that leads to autoignition is on the oxidizer side of the stagnation plane. The fuel diffuses through the stagnation plane to a zone where low-temperature reactions take place and form H_2O_2, peroxides and keto-hydroperoxides as well as heptenes and heterocycle compounds. These species, especially H_2O_2 diffuse further upstream towards the oxidizer boundary and facilitate the "hot"-ignition.

Figure 6 compares predicted values of critical conditions of autoignition for the surrogates with experimental data. In general the predictions agree well with measurements. At a given value of p, T_{ig} for the Aachen Surrogate is the lowest followed by Surrogate C and the Princeton Surrogate. The relative order of reactivity can be explained by consideration of the volatility and

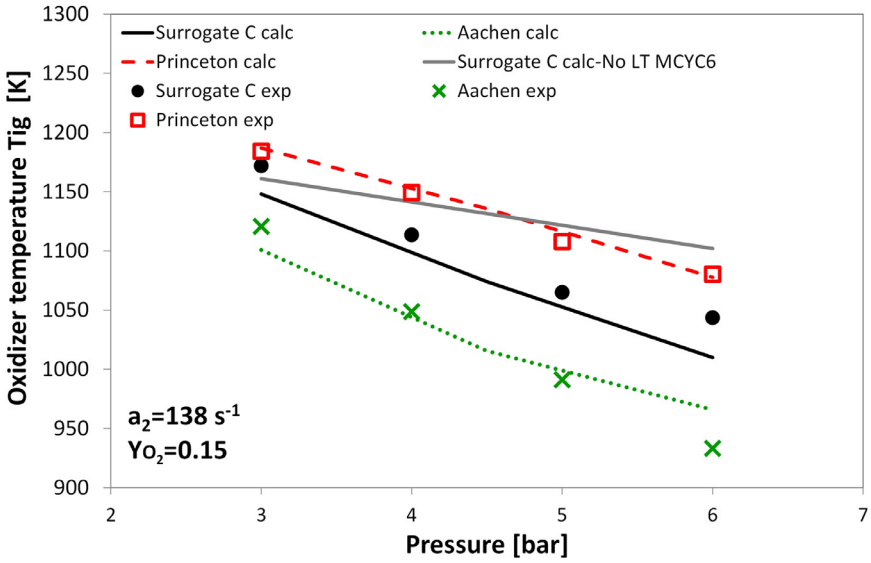

Fig. 6. The temperature of the oxidizer stream at autoignition, T_{ig} as a function of pressure, p, at $a_2 = 138\,s^{-1}$, and $Y_{O_2,2} = 0.15$. The symbols represent experimental data for the surrogates (same as those shown in Fig. 2) and the lines are predictions. The figure also shows predictions for Surrogate C obtained after removing reactions that characterize low-temperature chemistry of methylcyclohexane (Marked as calc-No LT MCYC6).

low-temperature reactivity of the components of the surrogates. A previous work has shown that for high-molecular weight hydrocarbon fuels autoignition is influenced by low-temperature chemistry at low strain rates while at high strain rates it is influenced by molecular transport [13], and the influence of low-temperature chemistry increases with increasing pressure [8]. The present work is at relatively low strain rates and elevated pressure, therefore autoignition can be expected to be influenced by low-temperature chemistry. The Aachen Surrogate is easiest to ignite because the value of T_s is highest among the surrogates tested. As a consequence large amounts of *n*-decane, that is known to have significant low-temperature reactivity [8,13], vaporizes from the surface leading to ignition. Surrogate C and the Princeton Surrogate have similar volatility but the components have different low-temperature reactivities. In particular, the presence of 2,2,4-trimethylpentane in the Princeton Surrogate (instead of methylcyclohexane as in Surrogate C) and of a larger amount of aromatics are responsible for its lower reactivity. Figure 6 shows that the reactivity of Surrogate C decreases if reactions that characterize low-temperature chemistry of methylcyclohexane are removed, and for a given p the difference between the predicted values of T_{ig} with and without low-temperature chemistry for methylcyclohexane increases with increasing pressure. This further highlights the influence of low-temperature reactivity of methylcyclohexane on autoignition.

Figures 7–9 show the sensitivity coefficients for the Aachen Surrogate, Surrogate C, and the Princeton Surrogate just before onset of "hot"-ignition. They show that autoignition is sensitive to reactions that characterize low and intermediate temperature chemistry [30] of the more volatile component in the surrogate. For example, the concentration of *n*-dodecane in the gas phase above the liquid pool of Surrogate C is about eight times smaller than that of methylcyclohexane, although *n*-dodecane is the largest constituent of this surrogate. As a consequence, autoignition of Surrogate C is mainly influenced by low-temperature chemistry of methylcyclohexane, and not that of the more reactive *n*-dodecane. The effect of *o*-xylene, which has a vapor pressure between those of the other two components, is also highlighted in the sensitivity analysis shown in Fig. 8. The influence of HO_2 is also evident from the sensitivities of its reactions shown in Figs. 7 and 8. It is formed in the NTC region, and the opposing influences of its termination step which forms H_2O_2, and its reactions with the benzylic type radicals of *o*-xylene and 1,3,5-trimethylbenzene that convert it into the more reactive OH, play major roles in determining ignition propensity [31]. Moreover, the decomposition of H_2O_2 is also a key reaction controlling the transition from NTC to high temperature ignition. For the same reasons, Fig. 7 shows that autoignition of Aachen Surrogate is primarily

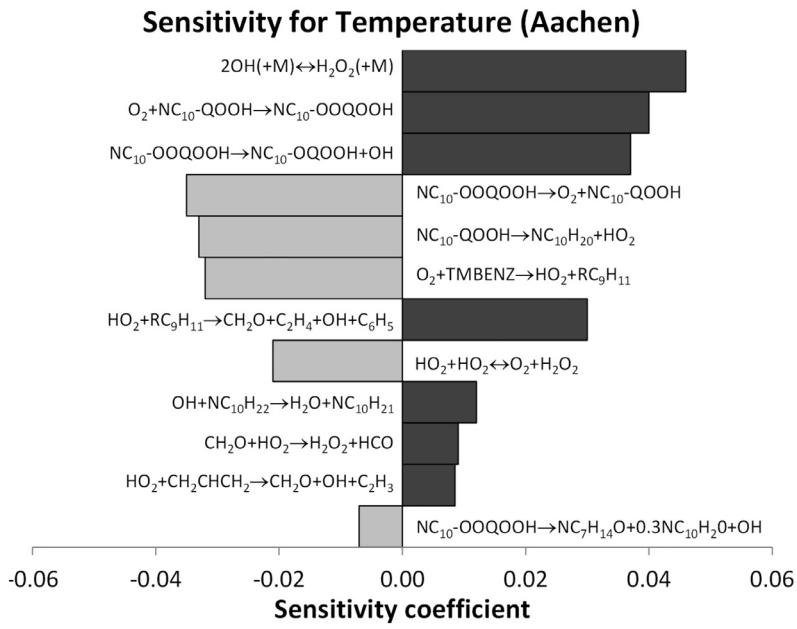

Fig. 7. Sensitivity coefficient for the Aachen Surrogate just before onset of "hot"-ignition at $p = 6$ bar, $Y_{O_2,2} = 0.15$, and $a_2 = 138\ s^{-1}$.

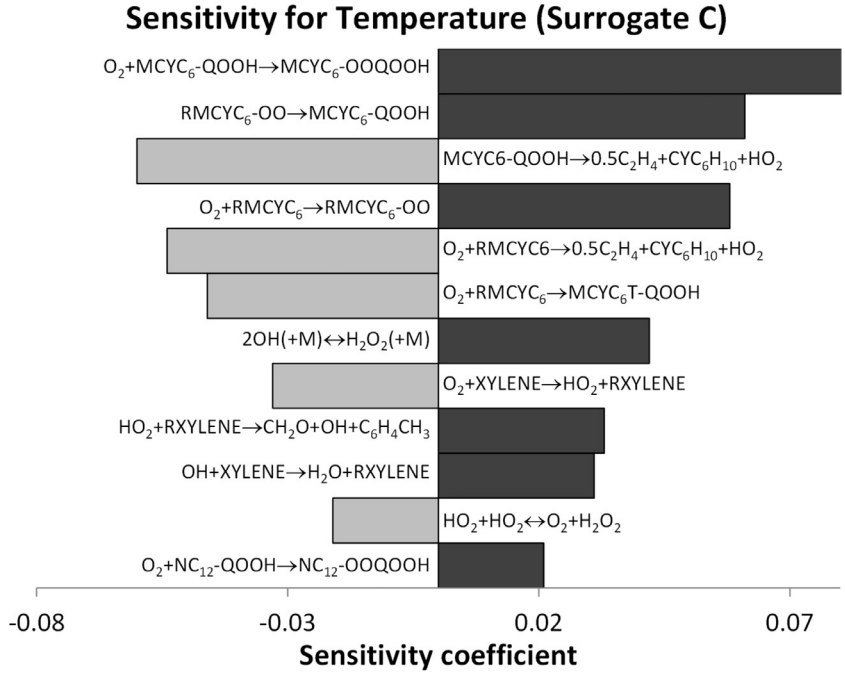

Fig. 8. Sensitivity coefficient for Surrogate C just before onset of "hot"-ignition at $p = 6$ bar, $Y_{O_2,2} = 0.15$, and $a_2 = 138\ s^{-1}$.

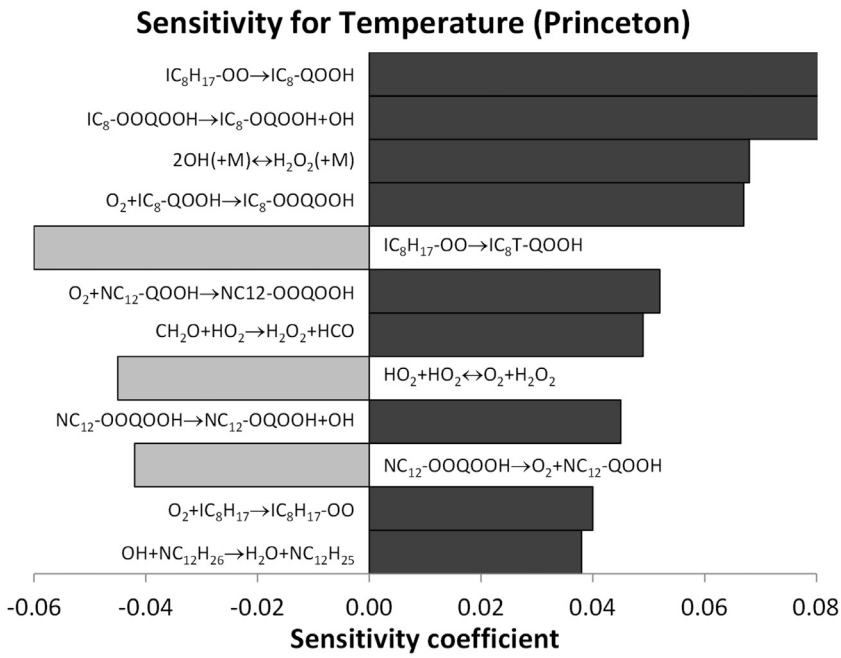

Fig. 9. Sensitivity coefficient for Princeton Surrogate just before onset of "hot"-ignition at $p = 6$ bar, $Y_{O_2,2} = 0.15$, and $a_2 = 138\ s^{-1}$.

influenced by low-temperature reactivity of *n*-decane. Beside being the main constituent of this surrogate, because its vapor pressure is close to that of 1,3,5-trimethylbenzene, its concentration is relatively high in the gas phase. Figure 9 shows that the critical condition of autoignition of the Princeton Surrogate is primarily influenced by 2,2,4-trimethylpentane as it is the most volatile component of this surrogate, despite the larger presence of the more reactive *n*-dodecane.

6. Concluding remarks

Experimental and computational studies described here show that the Aachen Surrogate, Surrogate C, and the 2nd generation Princeton Surrogate reproduce the critical conditions of autoignition of the jet fuels JP-8, and Jet-A reasonably well. The predictions of critical conditions of autoignition of the kinetic model are reasonably accurate. The computational study shows the dominant role played by low-temperature chemistry in promoting autoignition, and a noteworthy finding is that autoignition is promoted by the low-temperature chemistry of the most volatile component in the surrogate mixture. The investigation described here was restricted to low values of the strain rates and low values of $Y_{O_2,2}$. It would be of interest to test the influence of low-temperature chemistry on autoignition at higher values of strain rates, oxygen mass fraction, and pressure.

Acknowledgments

The authors acknowledge Professor F. A. Williams and Professor E. Ranzi for their contributions and helpful discussions. The research at UCSD is supported by the U. S. Army Research Office, Grant # W911NF-16-1-0054 (Program Manager Ralph A. Anthenien Jr). Politecnico di Milano has received funding from the European Union's Horizon 2020 research and innovation programme under grant agreement No 723525.

Supplementary material

Supplementary material associated with this article can be found, in the online version, at doi:10.1016/j.proci.2018.06.224.

References

[1] T. Edwards, L.Q. Maurice, *J. Propul. Power* 17 (2001) 461–466.
[2] S. Dooley, S.H. Won, J. Heyne, et al., *Combust. Flame* 159 (2012) 1444–1466.
[3] T. Malewicki, S. Gudiyella, K. Brezinsky, *Combust. Flame* 160 (2013) 17–30.
[4] K. Narayanaswamy, P. Pepiot, H. Pitsch, *Combust. Flame* 161 (2014) 866–884.
[5] Y. Zhu, S. Li, D.F. Davidson, R.K. Hanson, *Proc. Combust. Inst.* 35 (2015) 241–248.
[6] A. Smallbone, W. Liu, C. Law, X. You, H. Wang, *Proc. Combust. Inst.* 32 (2009) 1245–1252.

[7] R. Gehmlich, A. Kuo, K. Seshadri, *Proc. Combust. Inst.* 35 (2014) 937–943.
[8] G. Mairinger, A. Frassoldati, R. Gehmlich, et al., *Combust. Theory Model.* 20 (2016) 995–1009.
[9] S. Honnet, K. Seshadri, U. Niemann, N. Peters, *Proc. Combust. Inst.* 32 (2008) 485–492.
[10] S. Humer, R. Seiser, K. Seshadri, *J. Propul. Power* 27 (2011) 847–855.
[11] K. Seshadri, S. Humer, R. Seiser, *Combust. Theory Model.* 12 (2008) 831–855.
[12] G. Jomaas, X. Zheng, D. Zhu, C. Law, *Proc. Combust. Inst.* 30 (2005) 193–200.
[13] R. Grana, K. Seshadri, A. Cuoci, U. Niemann, T. Faravelli, E. Ranzi, *Combust. Flame* 159 (2012) 130–141.
[14] K. Seshadri, F.A. Williams, *Int. J. Heat Mass Transf.* 21 (2) (1978) 251–253.
[15] R. Seiser, *Nonpremixed Combustion of Liquid Hydrocarbon Fuels*, Technical University of Graz, 2000 Ph.D thesis.
[16] U. Niemann, K. Seshadri, F.A. Williams, *Proc. Combust. Inst.* 34 (2013) 881–886.
[17] U. Niemann, K. Seshadri, F.A. Williams, *Combust. Flame* 161 (2014) 138–146.
[18] F. Carbone, A. Gomez, *Proc. Combust. Inst.* 35 (2015) 761–769.
[19] L. Tosatto, F. Mella, M.B. Long, M.D. Smooke, *Combust. Flame* 159 (2012) 3027–3039.
[20] K. Seshadri, A. Frassoldati, A. Cuoci, et al., *Combust. Theory Model.* 15 (2011) 569–583.
[21] S. Humer, A. Frassoldati, S. Granata, et al., *Proc. Combust. Inst.* 31 (2007) 393–400.
[22] E. Ranzi, A. Frassoldati, A. Stagni, M. Pelucchi, A. Cuoci, T. Faravelli, *Int. J. Chem. Kinet.* 46 (2014) 512–542.
[23] A. Agosta, N.P. Cernansky, D.L. Miller, T. Faravelli, E. Ranzi, *Exper. Thermal Fluid Sci.* 28 (2004) 701–708.
[24] B.W. Weber, W.J. Pitz, M. Mehl, E.J. Silke, A.C. Davis, C.-J. Sung, *Combust. Flame* 161 (8) (2014) 1972–1983, doi:10.1016/j.combustflame.2014.01.018.
[25] A. Cuoci, A. Frassoldati, T. Faravelli, E. Ranzi, *Comput. Phys. Commun.* 192 (2015) 237–264.
[26] J.M. Smith, H.C.V. Ness, M.M. Abbott, *Introduction to Chemical Engineering Thermodynamics*, Fifth, Mc Graw Hill, 1996.
[27] D.W. Green, R.H. Perry, *Perry's Chemical Engineers' Handbook*, 8, McGraw Hill, 2008.
[28] A. Cuoci, A. Frassoldati, T. Faravelli, E. Ranzi, *Proc. Combust. Inst.* 35 (2015) 1621–1627.
[29] A. Frassoldati, G. D'Errico, T. Lucchini, et al., *Reduced kinetic mechanisms of diesel fuel surrogate for engine CFD simulations, Combust. Flame* 162 (2015) 3391–4007.
[30] J. Zádor, C.A. Taatjes, R.X. Fernandes, *Progress Energy Combust. Sci.* 37 (2011) 371–421.
[31] G. da Silva, J.W. Bozzelli, *Proc. Combust. Inst.* 32 (2009).